

See discussions, stats, and author profiles for this publication at: <https://www.researchgate.net/publication/2456815>

Exit Time approach for Lagrangian and Eulerian Turbulence

Article · August 1999

Source: CiteSeer

CITATIONS

2

5 authors, including:



Angelo Vulpiani

Sapienza University of Rome

395 PUBLICATIONS **12,873** CITATIONS

[SEE PROFILE](#)



Luca Biferale

University of Rome Tor Vergata

280 PUBLICATIONS **5,837** CITATIONS

[SEE PROFILE](#)



Antonio Celani

Abdus Salam International Centre for Theoretical Physics

144 PUBLICATIONS **3,467** CITATIONS

[SEE PROFILE](#)

Some of the authors of this publication are also working on these related projects:



Turbulence [View project](#)



Statistical Mechanics, Thermodynamics, Kinetic Theory [View project](#)

Exit Time approach for Lagrangian and Eulerian Turbulence

*A. Vulpiani*¹, *L. Biferale*², *G. Boffetta*³,
*A. Celani*³, *M. Cencini*¹ and *D. Vergni*¹

¹Dipartimento di Fisica and INFM, Università di Roma “La Sapienza”,
Piazzale Aldo Moro 2, I-00185, Roma, Italy

²Dipartimento di Fisica and INFM, Università di Roma “Tor Vergata”,
Via della Ricerca Scientifica 1, I-00133 Roma, Italy

³Dipartimento di Fisica Generale and INFM, Università di Torino,
Via Pietro Giuria 1, I-10125 Torino, Italy

Abstract

Usually, intermittency in turbulence is studied by looking at the scaling of structure functions of different orders versus time and space separation (Eulerian statistics) or by looking at different moments of particles distance versus time (Lagrangian statistics). Here, we discuss an alternative approach in which one analyses the statistical properties of the time necessary to have a fixed velocity fluctuation in the Eulerian case or a fixed distance separation in the Lagrangian case. This method gives good results also at low Reynolds numbers, where the traditional approach for both Eulerian or Lagrangian descriptions is not very accurate. In addition, the approach here proposed is able to catch the statistical properties of laminar fluctuations in turbulent flows.

1 Introduction

The understanding of Eulerian intermittency, i.e. the corrections to the prediction obtained with dimensional arguments according to the Kolmogorov 1941 approach, is one of the main goals of theoretical investigation of fully developed turbulence (Frisch 1995). A related problem is the effect of Eulerian intermittency on the Lagrangian properties, i.e. the corrections to the Richardson’ law for the relative dispersion (Richardson 1926, Novikov 1989). For a detailed introduction to the statistical mechanics of Eulerian and Lagrangian turbulence see Monin and Yaglom (1975), Frisch (1995), Bohr et al. (1998). Eulerian turbulence has attracted most of the attention in the last 20 years, while there are relatively few studies for the corresponding Lagrangian statistics (Novikov 1989, Borgas 1993, Boffetta et al. 1999a, Paret et al. 1998). The standard way to characterize Eulerian intermittency is the investigation

of the scaling properties of the structure functions, i.e. the moments of the velocity difference as function of the space separation (or time delay according to the Taylor hypothesis, e.g. in the case of one point velocity measurement by an anemometer). Similarly for the Lagrangian aspects one looks at the moments of the relative particle pairs distance as function of time.

The above usual methods work very well in the cases of very extended inertial range. Unfortunately, both in experimental and numerical context one has to deal with a limited scale separation which entails several practical difficulties that may originate ambiguous results.

In the last few years, in order to characterize the non-asymptotic properties of transport in realistic systems, e.g. closed basins where the typical Eulerian length is not very small compared with the domain size, an alternative approach has been proposed (Artale et al. 1997, Boffetta et al. 1999a). The basic idea is to fix a certain separation for a particle pair and to analyse the statistical properties of the time necessary for doubling its separation. The fixed scale method is able to give the proper description also in non-ideal cases, while whenever large-scale separations are involved it coincides with the usual analysis.

In Section 2 we introduce the concept of Finite Size Lyapunov Exponent and we show its application to relative diffusion in finite domains and for fully developed turbulence with the aid of synthetic velocity fields.

Section 3 is devoted to the investigation of the statistical properties of the time necessary to have a fixed velocity fluctuation of a turbulent signal, i.e. a sort of inverse structure function (Jensen 1999). This allows us for an unambiguous detection of the intermediate dissipative range (Biferale et al. 1999).

For the sake of completeness in Appendix A we report the basic elements of the multifractal model. Appendix B contains some details about the Finite Size Lyapunov Exponent.

2 Exit times for Lagrangian dynamics

2.1 Finite Size Lyapunov Exponent

Understanding the statistics of particle pairs dispersion is of fundamental interest in Lagrangian turbulence. At variance with absolute (one particle) dispersion, which is dominated by large scale flow, relative (two particle) dispersion is driven by the local velocity difference. Relative dispersion thus gives information on the velocity field structure at different scales. Nevertheless the reconstruction of the Eulerian properties from Lagrangian measurements is not a simple task (Monin and Yaglom 1975). This is due to the fact that, even in presence of a simple Eulerian velocity field, Lagrangian trajectories can display a very complex behaviour due to Lagrangian Chaos phenomenon

(Ottino 1989).

By definition, chaotic motion means exponential separation of close trajectories. Therefore, in presence of Lagrangian Chaos we expect that the relative separation between advected tracers, $R(t)$, typically grows exponentially in time. The exponential regime is observed only for separation $R \ll \eta$, where η is the characteristic scale of the smallest Eulerian structures (i.e. dissipative eddies in turbulence). For 3D homogeneous fully developed turbulence in the inertial range, $\eta \ll R(t) \ll L_0$ (being L_0 the typical scale of energy injection), one has the Richardson law, $\overline{R^2(t)} \propto t^3$. Hereafter $\langle \dots \rangle$ indicates the average over many particle pairs. For very large separations ($R \gg L_0$), the behaviour of $R(t)$ depends on the structure of the velocity field and one has the usual diffusive behaviour $\overline{R^2(t)} \sim Dt$, being D the diffusion coefficient.

In real settings, e.g. relatively small inertial range, the standard analysis at fixed delay time, i.e. to look at $\overline{R^2(t)}$ as a function of t , can lead to ambiguous results. The possibility to have at the same time particles pairs in range of scales having different dynamical and statistical properties, e.g. in turbulence in the dissipative range and in the inertial one (or in the inertial range and in the diffusive one), can produce long crossover effects which can be wrongly interpreted (Artale et al. 1997).

In the last few year, in order to overcome such difficulties we have developed an alternative approach which is based on the study of the fixed-scale statistics in spite of the fixed-time one. In particular, we have introduced an indicator, the Finite Size Lyapunov Exponent (FSLE), which is an extension of the Lyapunov exponent by computing averaged quantities at fixed scale (Aurell et al. 1996, 1997). Let us now recall the basic idea.

We define a series of thresholds $R_n = \rho^n R_0$, ($n = 1, \dots, N$) and we measure the “doubling times”, $T(R_n)$, it takes for the two particles separation, initially of size $R(0) \leq R_0$, to grow from R_n to R_{n+1} , until it reaches the largest scale under consideration R_N . The threshold rate, ρ , has to be larger than 1. However, we choose ρ not too large in order to avoid contributions coming from different scales.

Performing $\mathcal{N} \gg 1$ experiments with different initial conditions, we define the Finite Size Lyapunov Exponent as:

$$\lambda(R) = \frac{1}{\langle T(R) \rangle_\epsilon} \ln \rho, \quad (2.1)$$

$\langle (\dots) \rangle_\epsilon$ is the average on the doubling time experiments, which is different from the time average over a single realization (Appendix B). For very small separation (i.e. $R \ll \eta$) from (2.1) one recovers the standard Lagrangian Lyapunov exponent, i.e.

$$\lambda = \lim_{R \rightarrow 0} \lambda(R). \quad (2.2)$$

See Aurell et al. (1996, 1997) for a detailed discussion about these points. At very large scales, if there is a standard diffusive regime ($\overline{R^2(t)} \sim Dt$), one

has:

$$\lambda(R) \approx \frac{D}{R^2}. \quad (2.3)$$

Moreover, if the flow is turbulent, in the inertial range, between the two regimes (2.2) and (2.3) one has the Richardson law, i.e.

$$\lambda(R) \sim R^{-2/3}. \quad (2.4)$$

The fixed scale analysis allows us to extract physical information at different spatial scales avoiding some unpleasant consequences resulting from working at a fixed delay time t , see Artale et al. (1997).

The FSLE analysis has been demonstrated an useful tool for the analysis of Lagrangian data in several situations. For example, in experiments of particles dispersion in closed basins of size L_B , the diffusive behaviour is observable only if $\eta \ll L_B$. Of course, this is not always the case (Boffetta et al. 1999b). In the following we will describe the application of the FSLE analysis to the study of relative dispersion in turbulent flow and to the analysis of experimental data in a non-turbulent flow, in which complex Lagrangian trajectories appear due to chaotic advection.

2.2 Dispersion in synthetic turbulent fields

We consider now the relative dispersion of particles pairs advected by an incompressible, homogeneous, isotropic, fully developed turbulent field. The Eulerian statistics of velocity differences is characterised by the Kolmogorov scaling $\delta v(R) \sim R^{1/3}$, in the inertial range ($\eta \ll R \ll L_0$). Due to incompressibility, particles will typically diffuse away from each other (Cocke 1969, Orszag 1970). For separations less than η we have exponential separation of trajectories, whereas at separations larger than L_0 normal diffusion takes place. In the inertial range the average pair separation is not affected neither by large scale components of the flow, which simply sweep the pair, nor by small scale ones, which act incoherently and with low intensity. Accordingly, the separation $R(t)$ feels mainly the action of velocity differences $\delta v(R(t))$ at scale R . As a consequence of the Kolmogorov scaling the separation grows with the *Richardson law* (Richardson 1926, Monin and Yaglom 1975)

$$\overline{R^2(t)} \sim t^3. \quad (2.5)$$

However, some unclear behaviours are observed when the Reynolds number is not large enough. As a matter of facts, even at very high Reynolds numbers, the inertial range is still too small to observe the scaling (2.5) without any ambiguity (Fung et al. 1992). On the other hand, we shall show that FSLE statistics is effective already a relatively small Reynolds numbers.

In order to investigate the problem of relative dispersion in turbulent flows a practical tool is the use of synthetic turbulent fields (Elliot and Majda 1996,

Fung et al. 1992, Fung and Vassilicos 1998). In fact, by means of stochastic processes it is possible to build a velocity field which reproduces some of the statistical properties of velocity differences observed in real fully developed turbulence (Biferale et al. 1998). To overcome the difficulties related to the sweeping, we limit ourselves to a correct representation of two-point velocity differences. In this case, if one adopts the reference frame in which one of the two tracers is at rest in the origin (the so called Quasi-Lagrangian frame of reference), then the motion of the second particle is ruled by the velocity difference in this frame of reference, which has the same single time statistics of the Eulerian velocity differences (L’vov et al. 1997).

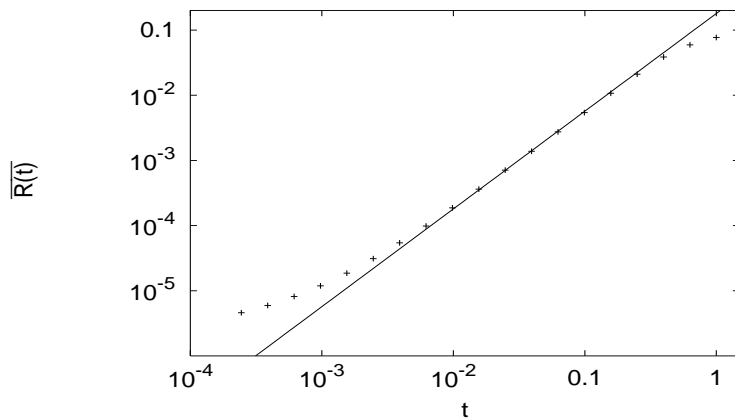


Figure 1: Relative dispersion $\overline{R(t)}$ versus time. Synthetic turbulent simulation averaged over 10^4 realizations. The line is the theoretical Richardson scaling $t^{3/2}$.

In Figure 1 we show the results of numerical simulations of pair dispersion in a synthetic turbulent field with the Kolmogorov scaling (i.e. with no intermittency) at Reynolds number $Re \simeq 10^6$ (Boffetta et al. 1999a). The expected power-law (2.5) can be observed without ambiguity only for huge Reynolds numbers. To explain the depletion of scaling range for the relative dispersion, let us consider a series of experiments, in which a couple of particles is released at a separation R_0 at time $t = 0$. At a fixed time t , as customarily is done, we perform an average over all different experiments to compute $\overline{R^2(t)}$. But, unless t is large enough that all particle pairs have “forgotten” their initial conditions, the average will be biased. This is at the origin of the flattening of $\overline{R^2(t)}$ for small times, which we can call a crossover from initial condition to self similarity. In an analogous fashion there is a crossover for large times (of the order of the integral time-scale) since some couples might have reached a separation larger than the integral scale, and thus diffuse normally, meanwhile other pairs still lie within the inertial range, biasing the average and, again, flattening the curve $\overline{R^2(t)}$. This correction to a pure power law is far from being negligible in experimental data, where

the inertial range is generally limited due to the relatively small value of the Reynolds number and the experimental apparatus. For example, Fung and Vassilicos (1998) and Fung (1992) show quite clearly the difficulties that may arise even in numerical simulations with the standard approach.

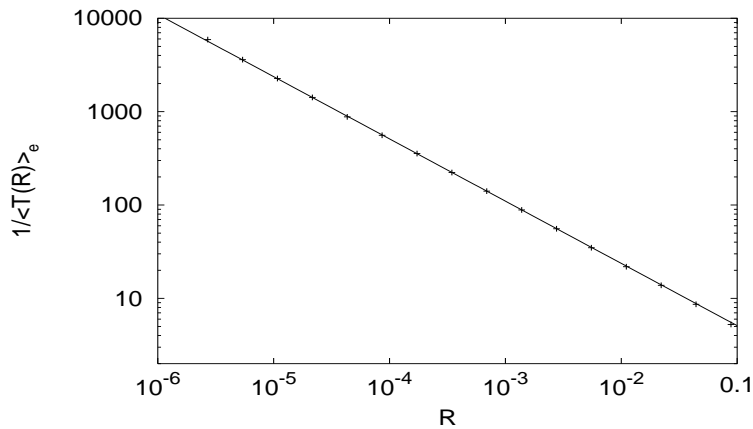


Figure 2: Average inverse doubling time $1/\langle T(R) \rangle_e$ for the same simulation of the Figure 1. Observe the enhanced scaling region. The line is the theoretical Richardson scaling $R^{-2/3}$.

To overcome these difficulties we exploit the approach based on the fixed scale statistics. The outstanding advantage of averaging at a fixed scale separation is that it removes all crossover effects, since all sampled pairs belong to the inertial range. The expected scaling properties of the doubling times is obtained by a simple dimensional argument. The time it takes for particle separation to grow from R to $2R$ can be estimate as $T(R) \sim R/\delta v(R)$; we thus expect the scaling

$$\frac{1}{\langle T(R) \rangle_e} \sim R^{-2/3} \quad (2.6)$$

In Figure 2 the great enhancement of the scaling range achieved by using the doubling times is evident. In addition, by using the FSLE it is possible to study in details the effect of Eulerian intermittency on the Lagrangian statistics of relative dispersion. See Boffetta et al. (1999a) for a detailed discussion in the framework of the multifractal model.

In conclusion we have that in this case doubling time statistics allows us a much better estimate of the scaling exponents with respect to the standard –fixed time– statistics.

2.3 Analysis of experimental data using the FSLE

Let us now discuss the use of the FSLE for the analysis of experimental Lagrangian data in a convective flow (Boffetta et al. 1999b). The experimental

apparatus is a rectangular convective tank $L = 15.0\text{ cm}$ wide, 10.4 cm deep and $H = 6.0\text{ cm}$ height filled with water. The upper and lower surfaces are kept at constant temperature and the side walls can be considered as adiabatic.

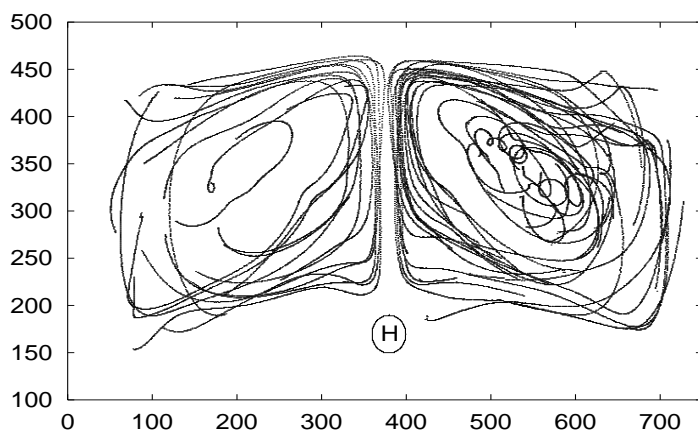


Figure 3: An example of trajectories reconstructed by the PVT technique (unit in pixels). The circle on the bottom represents the heater.

Convection is generated by an electrical circular heater, 0.8 cm in diameter, located in the mid-line of the tank, just above the lower surface (see Figure 3). The heater furnish a constant heat flux controlled by a feedback on the power supply.

The control parameter of the experiment is the Rayleigh number, Ra , which varies over a wide range of values. The geometrical configuration constrains the convective pattern to two counter-rotating rolls divided by a oscillating thermal plume (Miozzi et al. 1998). The Eulerian velocity field is thus, basically, two-dimensional and time periodic.

Lagrangian data are obtained by Particle Tracking Velocimetry (PTV) technique. Figure 3 shows an example of the output of the PTV analysis.

We report the result of the FSLE analysis applied to 6 different runs at different Rayleigh number. Each run consists of 22500 frames containing 900 simultaneous trajectories on average. In Figure 4 we show the FSLE for the run at $Ra = 2.39 \cdot 10^8$. In order to increase the statistics at large separations we performed the analysis with different initial threshold R_0 . For small R , we observe the collapse of $\lambda(R)$ to the value of the Lyapunov exponent, independent on R_0 .

For larger separation $\lambda(R)$ decreases to smaller values, indicating a slowing down in the separation growth due to the presence of boundaries. The behaviour of $\lambda(R)$ is well described by assuming exponential relaxation of $R(t)$ to the saturation value R_{max} (uniform distribution in the tank). The predic-

tion is (Artale et al. 1997)

$$\lambda(R) \simeq \frac{1}{\tau_R} \frac{R_{max} - R}{R}, \quad (2.7)$$

where τ_R is the characteristic relaxation time (see Appendix B).

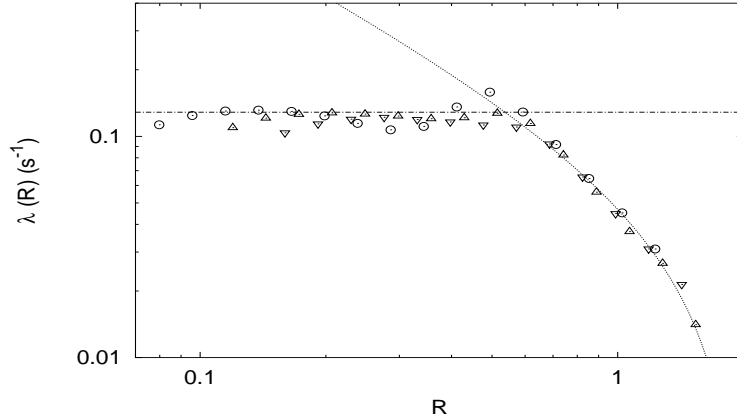


Figure 4: $\lambda(R)$ versus R for the run at $Ra = 2.39 \cdot 10^8$ and different initial threshold $R_0 = 0.4 \text{ cm}$ (\circ), $R_0 = 0.6 \text{ cm}$ (\triangle) and $R_0 = 0.8 \text{ cm}$ (∇). The straight line is the Lyapunov exponent $\lambda = (0.12 \pm 0.01) \text{ s}^{-1}$ and the curve represents the saturation regime (2.7).

We observe that in this experiment we cannot expect to observe diffusive behaviour because the size of Eulerian structure is of the same order of the tank size. Let us conclude by observing that in this case the FSLE analysis has given a clear evidence of Lagrangian Chaos (i.e. $\lambda > 0$) and, moreover, it has given a good description of the separation evolution on all the observable scales.

3 Exit times for turbulent signals and the Intermediate dissipative range

The most studied statistical indicators for intermittency in homogeneous isotropic turbulence are the longitudinal structure functions, i.e. moments of the velocity increments at distance R in the direction of $\hat{\mathbf{R}}$:

$$S_p(R) = \langle [(\mathbf{v}(\mathbf{x} + \mathbf{R}) - \mathbf{v}(\mathbf{x})) \cdot \hat{\mathbf{R}}]^p \rangle. \quad (3.1)$$

Basically in typical experiments one is forced to analyse one-dimensional string of data, e.g. the output of hot-wire anemometer. In these cases the Taylor Frozen-Turbulence Hypothesis is used to bridge measurements in space

with measurements in time. Within the Taylor Hypothesis, one has the large-scale typical time, $T_0 = L_0/U_0$, and the dissipative time, $t_d = \eta/U_0$, where U_0 is the large scale velocity field at the scale of the energy injection. As a function of time increment, τ , structure functions (3.1) assume the form: $S_p(\tau) = \langle [(v(t+\tau) - v(t))^p] \rangle$. It is well known that in the inertial range, $\tau_d \ll \tau \ll T_0$, the structure functions develop an anomalous scaling behaviour: $S_p(\tau) \sim \tau^{\zeta(p)}$, where $\zeta(p)$ is a non linear function, while inside the dissipative range, $\tau \ll \tau_d$, they show the laminar scaling: $S_p(\tau) \sim \tau^p$.

Beside the huge amount of theoretical, experimental and numerical studies devoted to the understanding of velocity fluctuations in the inertial range (Frisch 1995, Bohr et al. 1998), only few –mainly theoretical– attempts have focused on the Intermediate Dissipation Range (IDR), we just mention Frisch and Vergassola (1991), Jensen et al. (1991), Gagne and Castaing (1991), L’vov et al. (1997), Benzi et al. (1999). By IDR we mean the range of scales, $\tau \sim \tau_d$, between the inertial and the dissipative range (see Appendix A).

The very existence of the IDR is relevant for the understanding of many theoretical and practical issues. Among them we cite: the modelizations of small scales for optimising Large Eddy Simulations and the validity of the Refined Kolmogorov Hypothesis, i.e. the bridge between inertial and dissipative statistics.

Non-trivial IDR properties are connected to intermittent fluctuations in the inertial range. Namely, anomalous scaling laws, can be explained by assuming that velocity fluctuations in the inertial range are characterised by a spectrum of different local scaling exponents: $\delta_\tau v = v(t+\tau) - v(t) \sim \tau^h$ with the probability to observe at scale τ a value h given by $P_\tau(h) \sim \tau^{3-D(h)}$. This is the celebrated multifractal picture of the energy cascade (see Appendix A) which has been confirmed by many independent experiments (Frisch 1995, Bohr et al. 1998). Non-trivial dissipative statistics is generated by fluctuations of the dissipative cut-off τ_d (see Appendix A):

$$\tau_d(h) \sim \nu^{1/(1+h)}. \quad (3.2)$$

Here we present the measurement both in experimental and synthetic data of a set of observable which are able to highlight the IDR properties. The main idea is to take a one-dimensional string of turbulent data, $v(t)$, and to analyse the statistical properties of the exit times from a set of defined velocity-thresholds. Roughly speaking a kind of Inverse Structure Functions (Jensen 1999). This approach is rather naturally related to the fixed scale method discussed in section 2 to study the particle separation statistics.

This analysis allow us to give the first clear evidence of non-trivial intermittent fluctuations of the dissipative cut-off in turbulent signals.

Fluctuations of viscous cut-off are particularly important for all those regions in the fluid where the velocity field is locally smooth, i.e. the local fluctuating Reynolds number is small. In this case, the matching between non-linear and viscous terms happens at scales much larger than the Kolmogorov scale, $\tau_d \sim$

$\nu^{-3/4}$. It is natural, therefore, to look for observable which feel mainly laminar events. A possible choice is to measure the exit-time moments through a set of velocity thresholds. More precisely, given a reference initial time t_0 with velocity $v(t_0)$, we define $\tau(\delta v)$ as the first time necessary to have an absolute variation equal to δv in the velocity data, i.e. $|v(t_0) - v(t_0 + \tau(\delta v))| = \delta v$. By scanning the whole time series we recover the probability density functions of $\tau(\delta v)$ at varying δv from the typical large scale values down to the smallest dissipative values. Positive moments of $\tau(\delta v)$ are dominated by events with a smooth velocity field, i.e. laminar bursts in the turbulent cascade. Let us define the Inverse Structure Functions (Inverse-SF) as:

$$\Sigma_p(\delta v) \equiv \langle \tau^p(\delta v) \rangle . \quad (3.3)$$

It is necessary to perform the average over the time-statistics in a weighted way. This is due to the fact that by looking at the exit-time statistics we are not sampling the time-series uniformly, i.e. the higher the value of $\tau(\delta v)$ is, the longer it is detectable in the time series.

It is easy to realize (Aurell et al. 1996, 1997 and Appendix B) that the sequential time average of any observable based on exit-time statistics, $\langle \tau^p(\delta v) \rangle_\epsilon$, is connected to the uniformly-in-time multifractal average by the relation:

$$\langle \tau^p(\delta v) \rangle = \frac{\langle \tau^{p+1} \rangle_\epsilon}{\langle \tau \rangle_\epsilon} . \quad (3.4)$$

According to the multifractal description we suppose that, for velocity thresholds corresponding to inertial range values of the velocity differences, $\delta_{\tau_d} v \equiv v_m \ll \delta v \ll v_M \equiv \delta_{T_0} v$, the following dimensional relation is valid:

$$\delta_{\tau} v \sim \tau^h \quad \rightarrow \quad \tau(\delta v) \sim \delta v^{1/h} ,$$

where the probability to observe a value τ for the exit time is given by inverting the multifractal probability, i.e. $P(\tau \sim \delta v^{1/h}) \sim \delta v^{[3-D(h)]/h}$. Made this ansatz, the prediction for the Inverse-SF, $\Sigma_p(\delta v)$ evaluated for velocity thresholds within the inertial range is:

$$\Sigma_p(\delta v) \sim \int_{h_{\min}}^{h_{\max}} dh \delta v^{[p+3-D(h)]/h} \sim \delta v^{\chi(p)} \quad (3.5)$$

where the RHS has been obtained by a saddle point estimate :

$$\chi(p) = \min_h \{ [p + 3 - D(h)]/h \} . \quad (3.6)$$

Let us now consider the IDR properties.

For each p , the saddle point evaluation (3.6) selects a particular $h = h_s(p)$ where the minimum is reached. Let us also remark that from (3.2) we have an estimate for the minimum value assumed by the velocity in the inertial range given a certain singularity h : $v_m(h) = \delta_{\tau_d(h)} v \sim \nu^{h/(1+h)}$. Therefore, the

smallest velocity value at which the scaling (3.5) still holds depends on both ν and h . Namely, $\delta v_m(p) \sim \nu^{h_s(p)/(1+h_s(p))}$. The most important consequence is that for $\delta v < \delta v_m(p)$ the integral (3.5) is not any more dominated by the saddle point value but by the maximum h value still dynamically alive at that velocity difference, $1/h(\delta v) = -1 - \log(\nu)/\log(\delta v)$. This leads for $\delta v < \delta v_m(p)$ to a pseudo-algebraic law:

$$\Sigma_p(\delta v) \sim \delta v [p + 3 - D(h(\delta v))]/h(\delta v). \quad (3.7)$$

The presence of this p -dependent velocity range, intermediate between the inertial range, $\Sigma_p(\delta v) \sim \delta v^{\chi(p)}$, and the dissipative scaling, $\Sigma_p(\delta v) \sim \delta v^p$, is the IDR signature.

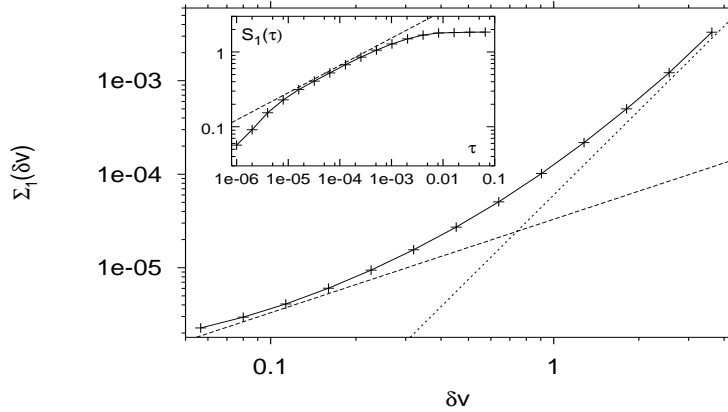


Figure 5: Inverse Structure Functions $\Sigma_1(\delta v)$. The straight lines shows the dissipative range behaviour (dashed) $\Sigma_1(\delta v) \sim \delta v$, and the inertial range non intermittent behaviour (dotted) $\Sigma_1(\delta v) \sim (\delta v)^3$. The inset shows the direct structure function $S_1(\tau)$ with superimposed the intermittent slope $\zeta(1) = .39$.

Then, it is easy to show that Inverse-SF should display an enlarged IDR. Indeed, for the usual *direct* structure functions the saddle point $h_s(p)$ value is reached for $h < 1/3$. This pushes the IDR to a range of scales very difficult to observe experimentally (Gagne and Castaing 1991). On the other hand, as regards the Inverse-SF, the saddle point estimate of positive moments is always reached for $h_s(p) > 1/3$. This is an indication that we are probing the laminar part of the velocity statistics. Therefore, the presence of the IDR must be felt much earlier in the range of available velocity fluctuations. Indeed, if $h_s(p) > 1/3$, the typical velocity field at which the IDR shows up is given by $\delta v_m(p) \sim \nu^{h_s(p)/(1+h_s(p))}$, that is much larger than the Kolmogorov value $\delta v_{\tau_d} \sim \nu^{1/4}$.

In Figure 5 we plot $\Sigma_1(\delta v)$ evaluated on a string of high-Reynolds number experimental data as a function of the available range of velocity thresholds

δv . This data set has been measured in a wind tunnel at $Re_\lambda \sim 2000$. One can see that the scaling is very poor. Indeed, it is not possible to extract any quantitative prediction about the inertial range slope. For this reason, we have only drawn the dimensional non-intermittent slope and the dissipative slope as a possible qualitative references. On the other hand, (inset of Figure 5), the scaling behaviour of the direct structure functions $\langle |\delta v(\tau)| \rangle \sim \tau^{\zeta(1)}$ is quite clear in a wide range of scales. This is a clear evidence of IDR's contamination into the whole range of available velocity values for the Inverse-SF cases. Similar results (not shown) are found for higher orders Σ_p structure functions.

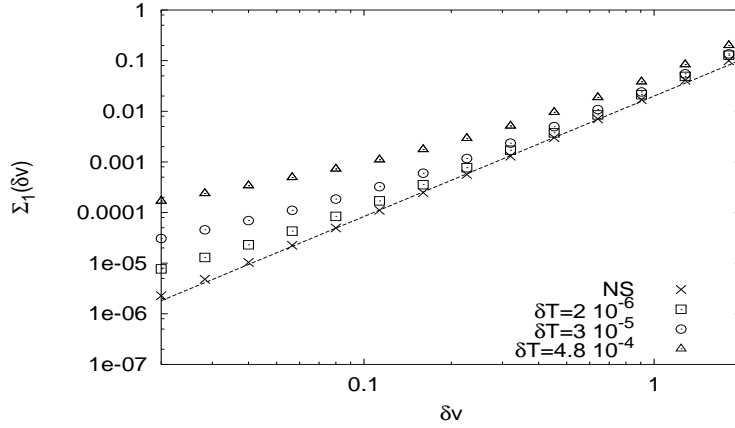


Figure 6: Inverse Structure Function $\Sigma_1(\delta v)$ versus δv for the synthetic signals not smoothed (*NS*) and smoothed with time windows: $\delta T = 4.8 \cdot 10^{-4}$, $3 \cdot 10^{-5}$, $2 \cdot 10^{-6}$, the straight line is obtained from the inverse multifractal prediction (3.6).

In order to better understand the scaling properties of $\Sigma_p(\delta v)$ we investigate a synthetic multiaffine field obtained by combining successive multiplications of Langevin dynamics (Biferale et al. 1998). The advantage of using a synthetic field is that one can control analytically the scaling properties of direct structure functions in order to have the same scaling laws observed in experimental data. An IDR can be introduced in the synthetic signals by smoothing the original dynamics on a moving time-window of size δT . Imposing a smoothing time-window is equivalent to fix the Reynolds number, $Re \sim \delta T^{-4/3}$. The purpose to introduce this stochastic multiaffine field is twofold. First we want to reach Reynolds numbers high enough to test the *inverse*-multifractal formula (3.6). Second, we want to test that the very extended IDR observed in the experimental data, see Figure 5, is also observed in this stochastic field. This would support the claim that the experimental result is the evidence of an extended IDR.

In Figure 6 we show the Inverse-SF, $\Sigma_1(\delta v)$, measured in the multiaffine synthetic signal at high-Reynolds numbers. The observed scaling exponent, $\chi(1)$,

is in agreement with the prediction (3.6). The same agreement also holds for higher moments.

In Table 1, we compare the best fit to the $\Sigma_p(\delta v)$ measured on the synthetic field with the inversion formula (3.6). As for the comparison between the theoretical expectation (3.6) and the synthetic data let us note the following points. First, in Biferale et al. (1998), it was proved that the signal possesses the correct direct-structure functions exponents for positive moments, i.e. the $\zeta(p)$ exponents are in a one-to-one correspondence with the $D(h)$ curve for $h < 1/3$. Nothing was proved for observable feeling the $h > 1/3$ interval. Therefore the agreement between the inversion formula (3.6) and the numerical results cannot be found analytically. Second, because the synthetic signal is defined by using Langevin processes, the less singular h -exponents expected to contribute to the saddle-point (3.6) is $h = 0.5$. Therefore, the theoretical prediction, $\chi_{th}(q)$, in Table 1 has been obtained by imposing $h_{max} = 0.5$.

Let us now go back to the most interesting question about the statistical properties of the IDR. In order to study this question we have smoothed the stochastic field, $v(t)$, by performing a running-time average over a time-window, δT . Then we compare Inverse-SF obtained for different Reynolds numbers, i.e. for different dissipative cut-off: $Re \sim \delta T^{-4/3}$.

The expression (3.7) predicts the possibility to obtain a data collapse of all curves with different Reynolds numbers by rescaling the Inverse-SF as follows Frisch and Vergassola (1991) and Jensen et al. (1991):

$$-\ln(\Sigma_p(\delta v))/\ln(\delta T/\delta T_0) \text{ vs. } -\ln(\delta v/U)/\ln(\delta T/\delta T_0), \quad (3.8)$$

where U and δT_0 are adjustable dimensional parameters.

Within the same experimental (or synthetic) set up they are Reynolds number independent (i.e. δT independent).

The rationale for the rescaling (3.8) stems from the observation that, in the IDR, $h_s(p)$ is a function of $\ln(\delta v)/\ln(\nu)$ only. Therefore, identifying $Re \propto \nu^{-1}$, the relation (3.8) directly follows from (3.7). This rescaling was originally proposed as a possible test of IDR for direct structure functions in Frisch and Vergassola (1991), but, as already discussed above, for the latter observable it is very difficult to detect any IDR due to the extremely small scales involved,

p	1	2	3	4	5
$\chi_{syn}(p)$	2.32(4)	4.40(8)	6.38(8)	8.3(1)	10.1(2)
$\chi_{th}(p)$	2.32	4.34	6.34	8.35	10.35

Table 1: Comparison between the Inverse-SF scaling exponents $\chi_{syn}(p)$ measured in the synthetic signal and the inversion of the theoretical multifractal prediction (3.6), $\chi_{th}(p)$. The synthetic signal has been defined such as the $D(h)$ function leads to the same set of experimental $\zeta(p)$ exponents for the direct structure functions.

as in Gagne and Castaing (1991).

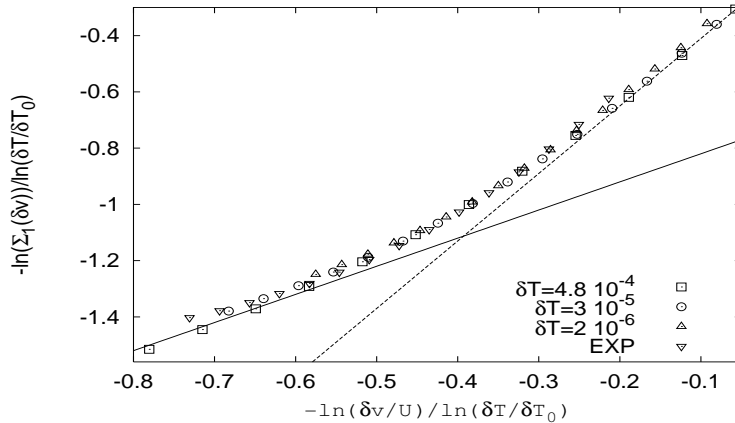


Figure 7: Data collapse of the Inverse-SF, $\Sigma_1(\delta v)$, obtained by the rescaling (3.8) for the smoothed synthetic signals (with time windows: $\delta T = 4.8 \cdot 10^{-4}$, $3 \cdot 10^{-5}$, $2 \cdot 10^{-6}$) and the experimental data (*EXP*). The two straight lines have the dissipative (solid line) and the inertial range (dashed) slope.

Figure 7 shows the rescaling (3.8) of the Inverse-SF, $\Sigma_1(\delta v)$, both for the synthetic field at different Reynolds numbers and for the experimental signals. As it is possible to see, the data-collapse is very good. This is a clear evidence that the poor scaling range observed in Figure 5 for the experimental signal can be explained as the signature of the IDR. The same behaviour holds for higher moments (not shown). It is interesting to remark that for a self-affine signal ($D(h) = \delta(h - 1/3)$), the IDR is highly reduced and the Inverse-SF, scaling trivially as $\Sigma_p(\delta v) \sim (\delta v)^{3p}$, do not bring any new information.

4 Concluding remarks

A new approach to look at Lagrangian and Eulerian statistical properties of turbulent flows has been reviewed. The main idea consists in looking at *inverse* scaling properties, i.e. looking at the time necessary to reach a certain (fixed) separation between advected particles instead of fixing the time and looking at the separations distribution for the Lagrangian aspects; or fixing the velocity increments and looking at the distribution of spatial separations where that fluctuations is detected for the Eulerian aspects.

In both cases some new and/or better statistical properties have been detected. First, for the Lagrangian properties, we have shown that the inverse statistics, based on the definition of “doubling-time” dramatically improves the scaling properties characterising the statistics of multi-point particles correlations in both ideal turbulent flows and realistic domain-bounded flows.

Second, for the Eulerian properties, the inverse statistics based on the concept of Inverse Structure Functions has revealed to be able to highlight the properties of the Intermediate-Dissipative-Range, a range of scales almost unaccessible by the usual direct Structure Functions.

Many questions are still open. As far as the Lagrangian approach is concerned, one can think to extend the preliminary attempts here presented to investigate realistic flows in a variety of different cases, going from geophysical flows to flows in closed laboratories. A sensible improvement in the quality of data analysis must certainly be expected.

In the Eulerian case, the analysis of a wider set of experimental data could make it possible to quantify the agreement of the data-collapse with the prediction based on (3.2) and (3.7). Indeed, it is easy to realize that, by using different parameterisation for the onset of the viscous range, one would have predicted the existence of an extended IDR for $\Sigma_p(\delta v)$ but with a slightly different rescaling procedure (Benzi et al. 1996). The quality of experimental data available to us is not high enough to distinguish between the two different predictions. Analysing different experimental data-sets, at different Reynolds numbers, could also make it possible to better explore $D(h)$ for $h > 1/3$ and thus to inquire possible non universalities of these $D(h)$ values. For example, as discussed above, in the Langevin synthetic-data a good agreement between the multifractal prediction and the numerical data is obtained by imposing $h_{max} = 0.5$, similarly in true turbulent data other h_{max} values could appear depending on the physical mechanism driving the energy transfer at large scales.

Acknowledgements

We thank U. Frisch, M.H. Jensen and M. Vergassola for useful suggestions and discussions. This work has been partly supported by INFM (*PRA-TURBO*) and by the European Network *Intermittency in Turbulent Systems* (contract number FMRX-CT98-0175).

Appendix A: Multifractal model for Turbulence

In the Kolmogorov (1941) theory of fully developed turbulence a global invariance with a fixed exponent $h_{k41} = 1/3$, is assumed:

$$|(\mathbf{v}(\mathbf{x} + \mathbf{R}, t) - \mathbf{v}(\mathbf{x}, t)) \cdot \mathbf{R}| \equiv \delta v_R(\mathbf{x}, t) \sim R^{h_{k41}} . \quad (4.1)$$

Relaxing this restrictive hypothesis, in the framework of multifractal model (Frisch 1995) one assumes that the velocity field possesses a local scale-invariance with a continuous spectrum of exponents, each of which belonging

to a given fractal set, Ω_h , with dimension $D(h)$:

$$\delta v_R(\mathbf{x}, t) \sim R^h \quad \text{for } \mathbf{x} \in \Omega_h \quad (4.2)$$

where $h \in (h_{\min}, h_{\max})$.

The probability to have a given scaling exponent h at the scale R is $P_R(h) \sim R^{3-D(h)}$, so the scaling of the structure function assumes the form:

$$S_p(R) = \langle (\delta v_R)^p \rangle \propto \int_{h_{\min}}^{h_{\max}} R^{hp} R^{3-D(h)} \mu(h) dh \sim R^{\zeta(p)} \quad (4.3)$$

where $\mu(h)$ is a smooth function independent of R . If $R \ll 1$, using a saddle point estimate one obtains

$$\zeta(p) \simeq \min_h \{hp + 3 - D(h)\} = h^*p + 3 - D(h^*) \quad (4.4)$$

being h^* solution of the equation $D'(h^*(p)) = p$ and $D''(h^*(p)) < 0$. Because of the Kolmogorov four-fifth law, one has $\zeta(3) = \min_h \{hp + 3 - D(h)\} = 1$. For the other moments, $\zeta(p)$, depends on the shape of $D(h)$, which cannot be obtained with simple arguments.

Frisch and Vergassola (1991), have shown that, in the context of the multifractal model of fully developed turbulence, it exists a non trivial behaviour of the structure functions in the region between the dissipative and the inertial range. In this range of scale, called intermediate dissipative range (IDR), the structure functions show a pseudo-algebraic scaling law, due to the fluctuations of the viscous cut-off. For a given scaling exponent h we can find the viscous cut-off, $\eta(h)$, for which the local Reynolds number is of order of unity:

$$\text{Re}(R) = \frac{R\delta v_R}{\nu} \sim O(1) \Rightarrow \eta(h) \sim \nu^{\frac{1}{(1+h)}}. \quad (4.5)$$

Taking into account the fluctuations of the cut-off the equation (4.3) assumes the form

$$S_p(R) \sim \int_{h_{\min}}^{h(R)} R^{hp+3-D(h)} \mu(h) dh \quad (4.6)$$

and therefore:

$$S_p(R) \propto \begin{cases} R^{\zeta(p)} & \text{if } R \gg \eta^* \\ R^{h(R)p+3-D(h(R))} & \text{if } \eta^* \gg R \gg \eta_{\min} \end{cases} \quad (4.7)$$

where η^* is the length scale related to the $h^*(p)$ (given by the saddle point evaluation) via $\eta^* = \nu^{\frac{1}{(1+h^*(p))}}$, $h(R)$ is the maximum exponent still present at the scale R for $\eta^* \gg R \gg \eta_{\min}$ given by $\nu^{\frac{1}{(1+h(R))}} = R$ and η_{\min} is the viscous cut-off related to the strongest singularity h_{\min} . If the saddle-point estimation, $h^*(p)$, is between $h(R)$ and h_{\min} then we have the usual scaling

relation. Vice versa if $h(R) > h^*(p)$ we are in the intermediate dissipative range and we have the pseudo algebraic scaling law.

A simple calculation shows that one has a universal function both in the inertial and in the IDR by introducing the multiscaling transformation. Let us discuss this for the energy spectrum $E(k) \sim k^{-1} S_2(R = k^{-1})$. Introducing the rescaled variables

$$F(\theta) = \frac{\ln E(k)}{\ln 1/\nu} \quad \text{and} \quad \theta = \frac{\ln k}{\ln 1/\nu} \quad (4.8)$$

from eq. (4.7) one obtains

$$F(\theta) \propto \begin{cases} -(1 + \zeta(2))\theta & \text{in the inertial range} \\ -2 - 2\theta + \theta D(h = -1 + 1/\theta) & \text{in the IDR} \end{cases} \quad (4.9)$$

The presence of the multiscaling behaviour was first experimentally verified by Gagne and Castaing (1991). However, since for $S_p(R)$ the extension of the IDR is very small, it is extremely difficult to have a strong evidence.

Appendix B: Finite Size Lyapunov Exponent

In this appendix we discuss the practical method for computing the Finite Size Lyapunov Exponent. Defined a norm for the distance $R(t)$ between two trajectories (two particles for relative dispersion), one defines a series of thresholds $R_n = \rho^n R_0$ ($n = 1, \dots, N$). Then one measures the time $T_\rho(R_n)$ that a perturbation of size R_n takes to grow up to R_{n+1} . The threshold rate ρ should not be taken too large to avoid growth on different scales. On the other hand, ρ cannot be too close to one, otherwise $T_\rho(R_n)$ would be of the order of the time step in the integration. Typically, one uses $\rho = 2$ or $\rho = \sqrt{2}$. For simplicity T_ρ is called ‘‘doubling time’’ even if $\rho \neq 2$.

The doubling times $T_\rho(R_n)$ are measured by following the evolution of the trajectories’ separation from its initial value $R_{min} \ll R_0$ up to the largest threshold R_N . One must choose $R_{min} \ll R_0$ in order to allow the direction of the initial perturbation to align with the most unstable direction in the phase-space. Moreover, one must pay attention to keep R_N smaller than the saturation distance, $R_N < R_{sat}$, so that all thresholds can be attained (R_{sat} is the typical distance of two uncorrelated trajectories).

The evolution of the error from the initial value, R_{min} , up to the largest threshold, R_N , carries out a single error-doubling experiment. At the end of each error-doubling experiment one rescales one trajectory at the initial distance R_{min} with respect to the other and starts another experiment. After \mathcal{N} error-doubling experiments, one can estimate the expectation value of some quantity A as:

$$\langle A \rangle_\epsilon = \frac{1}{\mathcal{N}} \sum_{i=1}^{\mathcal{N}} A_i. \quad (4.1)$$

The average $\langle (\dots) \rangle_e$ is not a time average: different error doubling experiments may take different times. Indeed we have

$$\langle A \rangle_t = \frac{1}{T} \int_0^T A(t) dt = \frac{\sum_i A_i \tau_i}{\sum_i \tau_i} = \frac{\langle A\tau \rangle_e}{\langle \tau \rangle_e}. \quad (4.2)$$

In the particular case in which A is the inverse of doubling time itself (as for compute the Lyapunov exponent) we have from (4.2)

$$\lambda(R_n) = \frac{1}{\langle T_r(R_n) \rangle_e} \ln \rho. \quad (4.3)$$

The above described method assumes that the distance between the two trajectories is continuous in time. For maps or for discrete sampling in time the method has to be slightly modified see Aurell et al. (1997).

Before concluding this Appendix, we discuss the behaviour of $\lambda(R)$ near the saturation, i.e. for distance of the order of the domain size. This behaviour mainly stems from the assumption that for large times the tracers tend to uniformly distribute in the domain and that small deviations from the asymptotic uniform distribution relax exponentially to that. This assumption is usually satisfied in generic chaotic dynamical systems even if it is difficult to prove. In the language of dynamical systems exponential relaxation to asymptotic distribution means that the second eigenvalue, α , of the Perron-Frobenius operator is inside the unitary circle, the relaxation time is $\tau_k = -\ln |\alpha|$ (see Ott (1993) for an introduction).

If the distribution relaxes exponentially to the uniform, the same should hold for the moment of the distribution. Therefore, for the large time evolution of the distance between two trajectories, $R(t)$, one expects:

$$R(t) \approx R_{max} - Ae^{-t/\tau_R} \quad (4.4)$$

being A and τ_R system-dependent. For $t \ll \tau_R$ or equivalently for $(R_{max} - R(t))/R(t) \ll 1$, one has:

$$\frac{d}{dt} \ln R = \lambda(R) = \frac{1}{\tau_R} \frac{R_{max} - R}{R}. \quad (4.5)$$

For an exact computation of eqs. (4.4-4.5) in a particular system see the appendix in Artale et al. (1997).

References

- Artale, V., Boffetta, G., Celani, A., Cencini, M., Vulpiani, A. (1997) "Dispersion of passive tracers in closed basins: Beyond the diffusion coefficient", *Phys. Fluids* **9**, 3162.

- Aurell, E., Boffetta, G., Crisanti, A., Paladin, G., Vulpiani, A. (1996) "Growth of non-infinitesimal perturbations in turbulence", *Phys. Rev. Lett.* **77**, 1262.
- Aurell, E., Boffetta, G., Crisanti, A., Paladin, G., Vulpiani, A. (1997) "Predictability in the large: an extension of the concept of Lyapunov exponent", *J. Phys. A* **30**, 1.
- Borgas, M. S. (1993) "The multifractal Lagrangian nature of turbulent", *Philos. Trans. R. Soc. London Ser. A* **342**, 379.
- Benzi, R., Paladin, G., Parisi, G., Vulpiani, A. (1984) "On the multifractal nature of fully developed turbulence and chaotic systems", *J. Phys. A* **17**, 3521.
- Benzi, R., Biferale, L., Ciliberto, S., Struglia, M.V., Tripiccion, R. (1996) "A generalized scaling of fully developed turbulence", *Physica D* **96**, 162.
- Benzi, R., Biferale, L., Ruiz-Chavarria, G., Ciliberto, S., Toschi, F. (1999) "Multiscale velocity correlations in turbulence: experiments, numerical simulations, synthetic signals", *Phys. Fluids* **11**, 2215.
- Biferale, L., Boffetta, G., Celani, A., Crisanti, A., Vulpiani, A. (1998) "Mimicking a turbulent signal: Sequential multi-affine processes", *Phys. Rev. E* **57**, R6261.
- Biferale, L., Cencini, M., Vergni, D., Vulpiani, A. (1999) "Exit time of turbulent signals: a way to detect the intermediate dissipative range", *chao-dyn/9904029*.
- Boffetta, G., Celani, A., Crisanti, A., Vulpiani, A. (1999a) "Relative dispersion in fully developed turbulence: Lagrangian statistics in synthetic flows", *Europhys. Lett.* **46**, 177
- Boffetta, G., Cencini, M., Espa, S., Querzoli, G. (1999b) "Chaotic advection and relative dispersion in a convective flow", in preparation.
- Bohr, T., Jensen, M.H., Paladin, G., Vulpiani, A. (1998) *Dynamical Systems Approach to Turbulence*, (Cambridge University Press, U.K.).
- Cocke, W.J. (1969) "Turbulent hydrodynamic line stretching: consequences of isotropy", *Phys. Fluids* **12**, 2488.
- Elliott, F.W. Jr., Majda, A.J. (1996) "Pair dispersion over an inertial range spanning many decades", *Phys. Fluids* **8**, 1052.
- Frisch, U., Vergassola, M. (1991) "A Prediction of the Multifractal Model: the Intermediate Dissipation Range." *Europhys. Lett.* **14**, 439.
- Frisch, U. (1995) *Turbulence. The legacy of A.N. Kolmogorov*, (Cambridge University Press, Cambridge).
- Fung, J.C.H., Vassilicos, J.C. (1998) "Two-particle dispersion in turbulent-like flows", *Phys. Rev. E* **57**, 1677.
- Fung, J.C.H., Hunt, J.C.R., Malik, N.A., Perkins, R.J. (1992) "Kinematic simulation of homogeneous turbulence by unsteady random Fourier modes" *J. Fluid Mech.* **236**, 281.
- Gagne, Y., Castaing, B. (1991) "Une représentation universelle sans invariance globale d'échelle des spectres d'énergie en turbulence développée" *C. R. Acad. Sci. Paris* **312**, 441.

- Jensen, M.H., Paladin, G., Vulpiani, A. (1991) "Multiscaling in Multifractals" *Phys. Rev. Lett.* **67**, 208.
- Jensen, M.H. (1999) "Multiscaling and Structure Functions in Turbulence: An Alternative Approach" *Phys. Rev. Lett.* **83**, 76.
- L'vov, V.S., Podivilov, E., Procaccia, I. (1997) "Temporal multiscaling in hydrodynamic turbulence", *Phys. Rev. E* **55**, 7030.
- Miozzi, M., Querzoli, G., Romano, G.P. (1998) "The investigation of an unstable convective flow using optical methods" *Phys. Fluids* **10**, 2995.
- Monin, A., Yaglom, A. (1975) *Statistical Fluid Mechanics* (MIT Press, Cambridge, Mass.), Vol. 2.
- Novikov, E.A. (1989) "Two-particle description of turbulence, Markov property and intermittency" *Phys. Fluids A* **1**, 326.
- Orszag, S.A. (1970) "Comment on: Turbulent hydrodynamic line stretching: consequences of isotropy", *Phys. Fluids* **13**, 2203.
- Ott, E. (1993) *Chaos in Dynamical Systems* (Cambridge University Press).
- Ottino, J.M. (1989) *The kinematics of mixing: stretching, chaos and transport* (Cambridge University Press).
- Paret J., Tabeling P. (1998) *Intermittency in two-dimensional inverse cascade of energy : experimental observations.* *Phys. Fluids* **10**, 3126.
- Richardson, L.F. (1926) "Atmospheric diffusion shown on a distance-neighbor graph", *Proc. Roy. Soc. A* **110**, 709.